

Resilience of spatial networks with inter-links behaving as an external field

Jingfang Fan,¹ Gaogao Dong,^{2,3,4} Louis M. Shekhtman,¹ Dong
Zhou,¹ Jun Meng,¹ Xiaosong Chen,^{5,6} and Shlomo Havlin¹

¹*Department of Physics, Bar Ilan University, Ramat Gan 52900, Israel*

²*Institute of applied system analysis, Faculty of Science,
Jiangsu University, Zhenjiang, 212013 Jiangsu, China*

³*Energy Development and Environmental Protection Strategy Research Center,
Faculty of Science, Jiangsu University, Zhenjiang, 212013 Jiangsu, China*

⁴*Center for Polymer Studies and Department of Physics,
Boston University, Boston, MA 02215, USA*

⁵*CAS Key Laboratory of Theoretical Physics, Institute of Theoretical Physics,
Chinese Academy of Sciences, Beijing 100190, China*

⁶*School of Physical Sciences, University of Chinese Academy of Sciences, Beijing 100049, China*

(Dated: January 21, 2022)

Abstract

Many real systems such as, roads, shipping routes, and infrastructure systems can be modeled based on spatially embedded networks. The inter-links between two distant spatial networks, such as those formed by transcontinental airline flights, play a crucial role in optimizing communication and transportation over such long distances. Still, little is known about how inter-links affect the resilience of such systems. Here, we develop a framework to study the resilience of interlinked spatially embedded networks based on percolation theory. We find that the inter-links can be regarded as an external field near the percolation phase transition, analogous to a magnetic field in a ferromagnetic-paramagnetic spin system. By defining the analogous critical exponents δ and γ , we find that their values for various inter-links structures follow Widom's scaling relations. Furthermore, we study the optimal robustness of our model and compare it with the analysis of real-world networks. The framework presented here not only facilitates the understanding of phase transitions with external fields in complex networks but also provides insight into optimizing real-world infrastructure networks and a magnetic field in a management.

I. INTRODUCTION

Robustness is of crucial importance in many complex systems and plays an important role in mitigating damage [1]. It has been studied widely in both single networks [2–4], interdependent networks [5–10] and multiplex networks [11, 12]. Percolation theory has demonstrated its great potential as a versatile tool for understanding system resilience based on both dynamical and structural properties [13, 14], and has been applied to many real systems [15–17]. Recently, a theoretical framework has been developed to study the resilience of communities formed of either Erdős-Rényi (ER) and Scale-Free networks that have inter-links between them using percolation theory [18]. It has been found that the inter-links affect the percolation phase transition in a manner similar to an external field in a ferromagnetic-paramagnetic spin system. However, many real systems, such as, transportation networks [19, 20], infrastructure networks [21] and others, are spatially embedded and the influence of this feature has not been considered. Here we study how the inter-links (e.g. air flights) between two spatial networks (e.g., countries) affect the overall resilience. Furthermore, we will search for an optimal structure (or most robust point) of our model and consider it in a real transportation system. We will do so by developing a framework to study the resilience of spatial networks with inter-links and by analysing possible optimal structures for our model/s and in real transport systems.

The structure of our paper is as follows: in the next Chapter, we describe and introduce the model. In Chapter III, the results are presented and discussed. Finally, in Chap. IV a short summary and outlook are provided.

II. MODEL

Our model is motivated by many real-world networks where nodes and links are spatially embedded within the same region (module), but only some nodes have connections to other regions (modules). We denote the links in the same module as *intra*links and the links between different modules as *inter*links. Fig. 1(a) demonstrates the topological structure of the global transportation network including railway roads and airline routes [22]. We demonstrate in the figure that the airports are connected via interlinks and can be regarded as *interconnected nodes*. We show here that

the interlinks behave, regarding breakdown of the network, in a manner analogous to an external field from physics near magnetic-paramagnetic phase transition [23, 24]. To study this effect, for simplicity and without loss of generalization, we carried out extensive simulations on a network of two modules each with the same number of nodes, $N_1 = L \times L$, where L is the linear size of the lattice, representing the spatial networks. Within each module the nodes are only connected with their neighbors in space as defined by a 2-dimensional square lattice. Between different modules, we randomly select a fraction r of nodes to be interconnected nodes, e.g, airports, and randomly assign M_{inter} interlinks among nodes in the two modules. A network generated from our model is shown in Fig. 1(b). Our model is realistic and can represent coupled transport systems, i.e, the nodes in the same lattice module are localized railroad or road networks within the same region while the interlinks represent interregional airline routes.

To quantify the resilience of our model, we carried out extensive numerical simulations of the size of the giant connected component $S(p, r)$ after a fraction of $1 - p$ nodes are randomly removed. Note that our model is distinct from the case of interdependent networks [5], where the failure of nodes in one network leads to the failure of dependent nodes in other networks. Our model is also different from the interconnected modules model [25], where interconnected nodes are attacked. In our model, the interconnections between different communities are additional connectivity links [26] and randomly chosen nodes are attacked [18]. For a given set of parameters $[p, r; L]$, we carried out 10,000 Monte Carlo realizations and took the average of these results to obtain $S(p, r)$.

III. RESULTS

Similar to our earlier studies [18, 27], we find that the parameter r , governing the fraction of interconnected nodes, has effects analogous to a magnetic field in a spin system, near criticality. This analogy can be seen through the facts that: (i) the non-zero fraction of interconnected nodes destroys the original phase transition point of the single module; (ii) critical exponents (defined below) of values derived from percolation theory can be used to characterize the effect of external field on $S(p, r)$. Fig. 2(a) shows our simulation results for the size of the giant component $S(p, r)$ with $L = 4096$, $M_{inter} = 2 \times L \times L$ for various r . We note that in the limit of $r = 0$ our model recovers the critical threshold of single square lattices, $p_c \approx 0.592746$ [28]. We find that

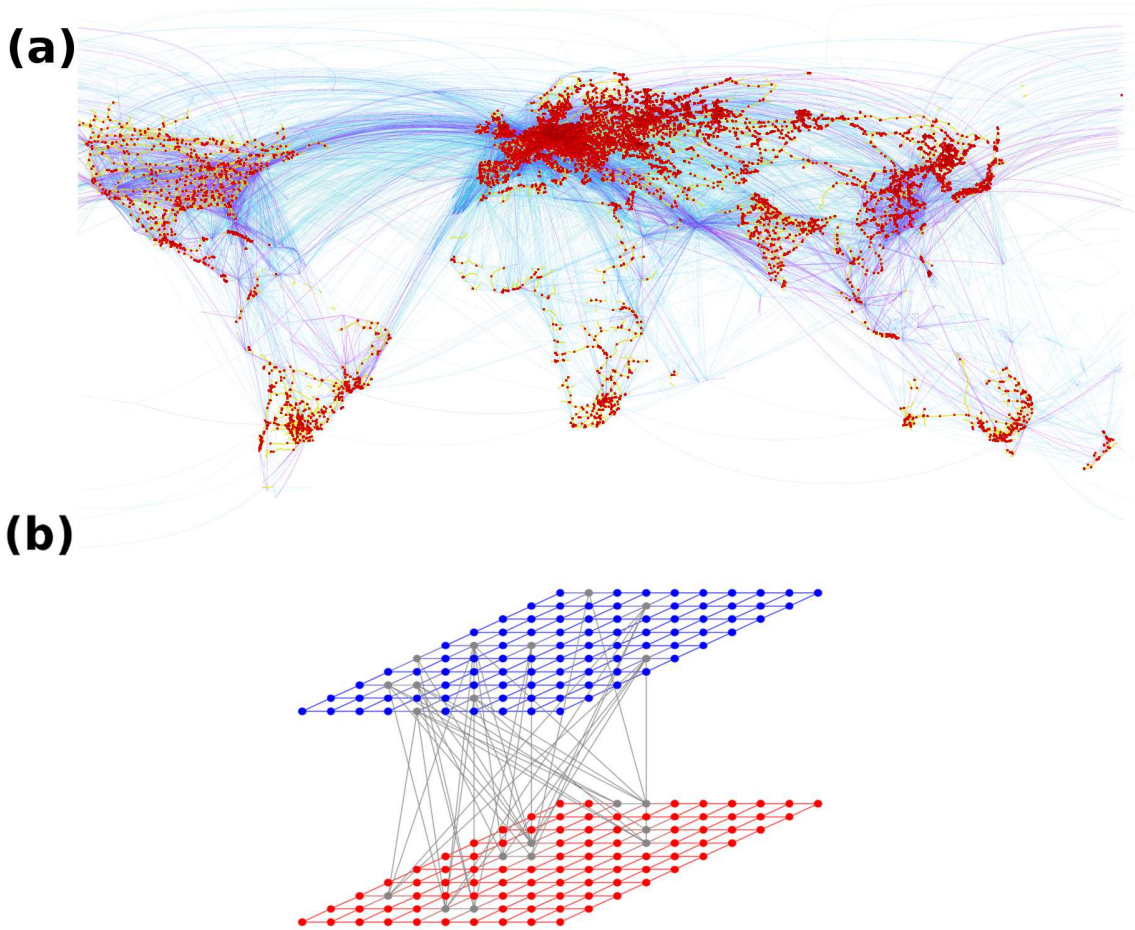


Figure 1. (a) The topological structure of the global transport network. The yellow links are railway lines, the red nodes are railway intersections, and the blue lines are global airline routes. (b) Our model. We assume two separate lattice networks, representing two continents (or countries) with railway networks. We add M_{inter} inter-links to a fraction r of nodes, representing cities with airports having flights to the other continent. Interconnected nodes and their respective interlinks are highlighted in gray. Here, we chose $r = 0.1$ and $M_{inter} = 50$.

$S(p_c, r) > S(p_c, 0) = 0$ for $r > 0$, showing that the interconnected nodes remove the phase transition of the single lattice.

Next, we investigate the scaling relations and critical exponents, with $S(p, r)$, p and r serving as our analogy for magnetization (order parameter), temperature, and the external field respectively

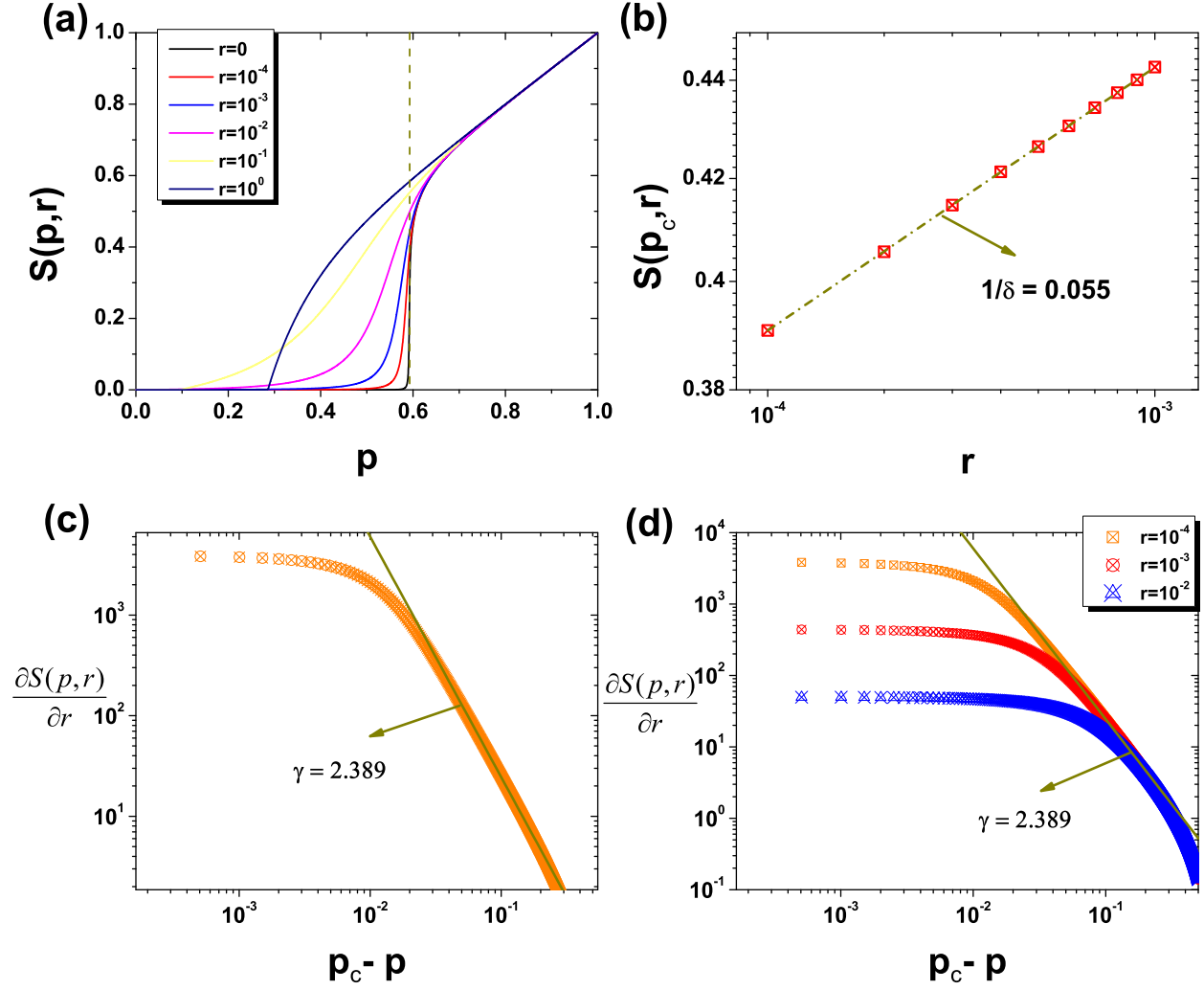


Figure 2. (a) The giant component (order parameter), $S(p, r)$, as a function of the fraction of non-removed nodes p for several values of r ; (b) $S(p_c, r)$ as a function of r with the exponent δ ; (c) $\frac{\partial S(p, r)}{\partial r}$ as a function of $p_c - p$ with $r = 10^{-4}$ and the exponent γ ; (d) Same as (c) but for several r . Here, $L = 4096$, $M_{inter} = 2 \times L \times L$, $p_c = 0.592746$. The dashed line is the best fit-line for the data, which is found to have a slope $1/\delta = 0.055$ and R-Square > 0.999 .

[23]. To quantify how the external field, r , affects the phase transition, we define the critical exponents δ , which relates the order parameter at the critical point to the magnitude of the field,

$$S(p_c, r) \sim r^{1/\delta}, \quad (1)$$

and γ , which describes the susceptibility near criticality,

$$\left(\frac{\partial S(p, r)}{\partial r}\right)_{r \rightarrow 0} \sim |p - p_c|^{-\gamma}, \quad (2)$$

where p_c is the site percolation threshold for a single 2-dimensional square lattice network.

The simulation results for δ in our model are shown in Fig. 2(b). We obtain $1/\delta = 0.055$ from simulations, which agrees very well with the known exponent value for standard percolation on square lattices $1/\delta = 5/91$ [13, 14]. The dashed line is the best fit-line for the data with R-Square > 0.999 .

We next investigate the critical exponent, γ , which we claim to be analogous to magnetic susceptibility exponent with the scaling relation given in Eq. (2). Fig. 2(c) presents our results for γ . We obtain $\gamma = 2.389$ for $p < p_c$ and $r = 10^{-4}$, which agrees again very well with the known value $\gamma = 43/18$ in percolation [13, 14]. In Fig. 2(d) we also plot our results for different r values: $r = 10^{-4}, 10^{-3}, 10^{-2}$ to highlight the changes in the range of the scaling region. We find that as r decreases, the scaling region becomes larger, this is expected since for smaller r the system approaches closer to criticality ($r=0$). Similar effects in terms of the scaling range are also observed for changing M_{inter} with respect to the critical exponent $1/\delta$ and Eq. (1), as seen in Fig. S1 [29].

We note that for a single 2d square lattice, the scaling exponent β , defined by the relation $S \sim (p - p_c)^\beta$, has a value of $\beta = 5/36$ [13, 14]. The critical exponent β together with δ and γ characterize the percolation universality class for our model. Since the various thermodynamic quantities are related, these critical exponents are not independent, but rather can be uniquely defined in terms of only two of them [30]. We find that the scaling hypothesis is also valid for our model and note that our values for these exponents are consistent with the Widom's identity $\delta - 1 = \gamma/\beta$ [14].

In the following, we test our framework on a real world example involving global transportation networks. We consider two railway networks, one in Europe (EU) and the other in North America (NA). The two railway networks have $N_{EU} = 8354$ and $N_{NA} = 933$ nodes (stations), as well as $M_{EU} = 11128$ and $M_{NA} = 1273$ intralinks respectively. As an example of adding long distance flights, we added M_{flight} interconnected links randomly among r fraction of the nodes (airport hubs). We used $M_{flight} = 1864$, which is the actual number of direct flights between the two continents. Fig. 3 shows our results for the system of the two real networks. We find that, the

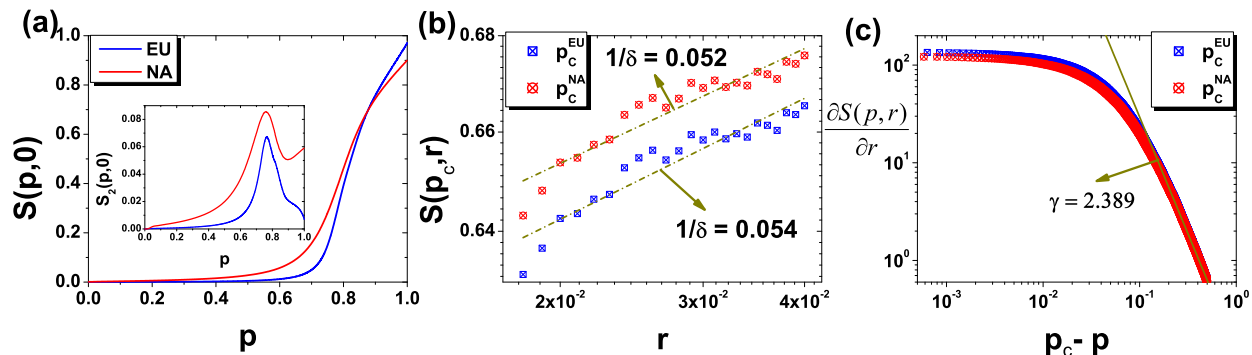


Figure 3. (a) $S(p, 0)$, versus the fraction of non-removed nodes, p , for real-data of the European (EU) and North America (NA) railway networks; (b) $S(p_c, r)$ as a function of r ; (c) $\frac{\partial S(p, r)}{\partial r}$ as a function of $p_c - p$ for $r = 10^{-2}$. Inset in (a) shows the second largest component $S_2(p, 0)$ as a function of p . We obtain our values of p_c based on the peak of $S_2(p, 0)$, which gives $p_c^{EU} = 0.7641$ and $p_c^{NA} = 0.7578$. The dashed lines in (b) are the best-fit lines for the data with slopes $1/\delta = 0.054$, $1/\delta = 0.052$ and R-Square > 0.89 . The network sizes are $N_{EU} = 8354$, $M_{EU} = 11128$; $N_{NA} = 933$, $M_{NA} = 1273$, $M_{flight} = 1864$.

values of the critical exponents δ and γ for the real networks [Fig. 3(b) and (c)] are consistent with the results obtained from our model. One should note that the percolation threshold p_c is different in each module when they are separated, since the number of nodes and links is not the same in both modules. To obtain the percolation threshold, p_c for each real railway network, we analyzed the second largest component, $S_2(p, 0)$. The size of the second largest cluster is known to be at a maximum at p_c [31]. We obtained $p_c^{EU} = 0.764$ and $p_c^{NA} = 0.758$ by utilizing the peak of $S_2(p, 0)$ for the EU and NA networks respectively [see inset of Fig. 3(a)].

To analyze the robustness of our model, we define an effective percolation threshold, p_{cut} , by using a small cut-off value of the giant component S_{cut} , as shown in Fig. 4(a). The threshold p_{cut} is defined as the point where $S(p, r)$ reaches S_{cut} . We assume that when $S(p, r)$ is very small as S_{cut} or below it is not functional. Interestingly, we find an optimal r in our model. It means that for a certain $r = r_{opt}$ the system is most robust i.e., p_{cut} is minimal. Indeed, Fig. 4(b) shows a specific example with $S_{cut} = 0.01$, where we find the optimal point to be $r_{opt} \approx 0.05$. In our framework, this suggests that if 5% of the cities have interconnected flights the network is most robust to random failures. The origin of this optimization phenomenon is due to the percolation

competition between the individual lattice module and the interconnected ‘network’ composed of r interconnected nodes/inter-links. When r is small enough, the behavior of the giant component $S(p, r)$ is dominated by the single lattice module [see Fig. 4(a)], and the threshold p_{cut} is large and close to p_c [see Fig. 4(b), with small r]; when r is increasing, the effect of the giant component of a single lattice module becomes weaker, but the effect from the interconnected nodes/inter-links becomes stronger resulting the decreasing of p_{cut} ; however, when r is large, the behavior of the giant component is dominated by the interconnected nodes/inter-links, p_{cut} is proportional to r [see Fig. 4(b), with large r]. In particular, our model will become like a random network, when $r = 1$. We also find that, in Fig. 4(b), there are no significant finite-size effects for our system since the three curves with $L = 1024, 2048, 4096$ are nearly overlapping. The results on how p_{cut} changes with S_{cut} and r are shown in Fig. 4(c).

Fig. 5(a) presents how p_{cut} changes with S_{cut} and r for a real network. These results are qualitatively similar to our model results [Fig. 4(c)]. We also observe that there exists an optimal value of r in the real transportation network. Fig. 5(b) shows three specific cases with $S_{cut} = 0.01, 0.05, 0.1$. We find that the optimal point is around $r_{opt} \approx 0.01$. Suggesting that if 1% of cities have inter-continental flights the system is optimally robust against random failures. For comparison, we also show in the figure the fraction of interconnected nodes in the real data: $r_{EU} = 0.0055$ and $r_{NA} = 0.05$. The lower and upper boundaries of the shadow in Fig. 5(b) are based on these two values.

Note that the number of interconnected links, M_{inter} , is kept constant when we change r in our model, i.e., $\langle k_{inter} \rangle$ is proportional to $1/r$. We also performed the same analysis to identify how the external field affects the resilience, i.e., the critical exponents δ, γ and effective percolation threshold of the spatial and ER networks when $\langle k_{inter} \rangle$ is fixed and M_{inter} changes, according to $\langle k_{inter} \rangle = \langle M_{inter} \rangle / (rN)$. The results are presented and discussed in Supplemental Materials [29].

IV. SUMMARY

We have developed a framework to study the resilience of coupled spatial networks where we show that the inter-links act analogously to an external field in a magnetic-paramagnetic system. Using percolation theory we studied the dynamical evolution of the giant component, and found

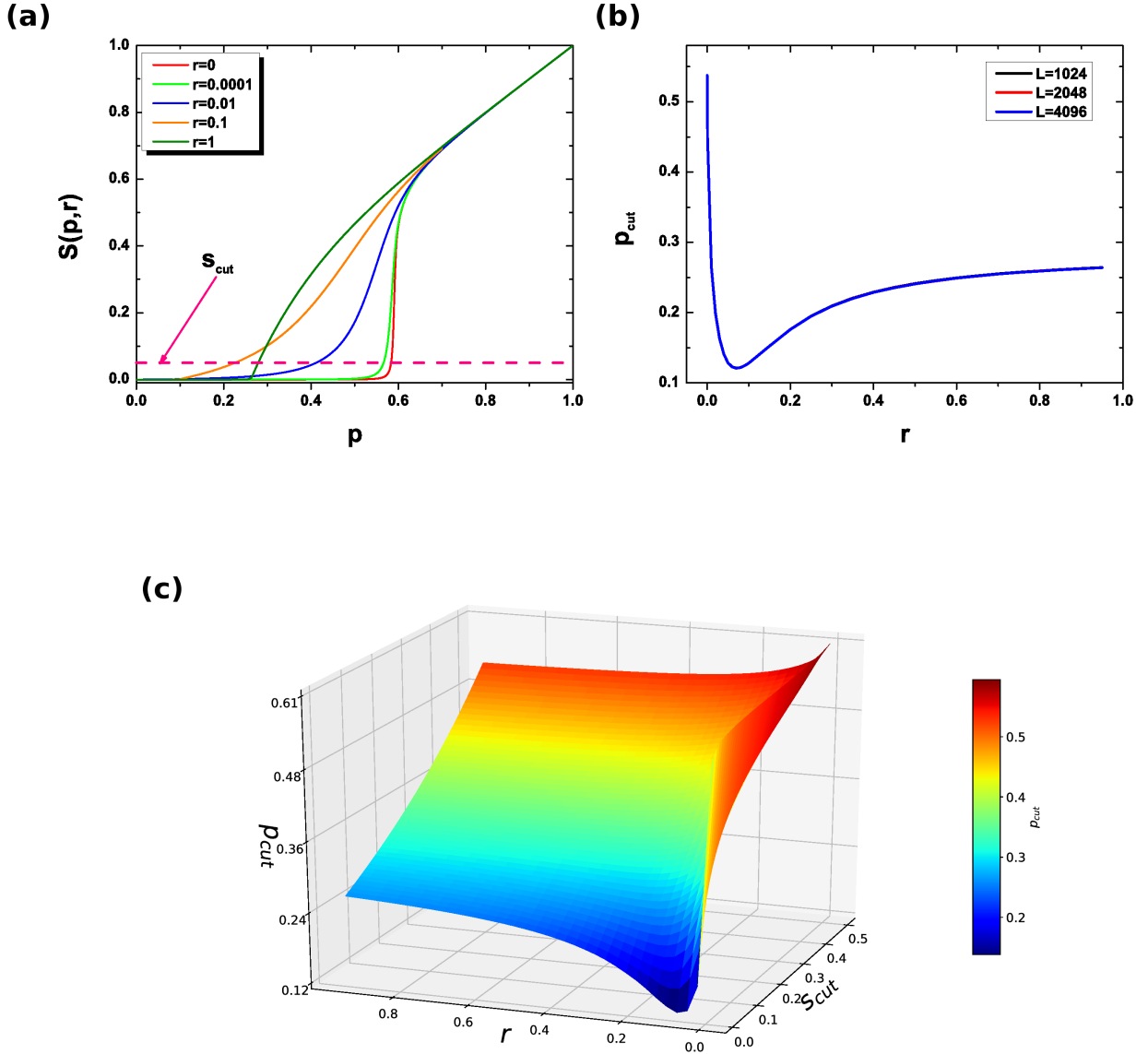


Figure 4. The effective percolation threshold, p_{cut} , for our model. (a) Definition of p_{cut} as the intersection between $S(p, r)$ and S_{cut} . (b) p_{cut} as a function of r with $S_{cut} = 0.01$. (c) p_{cut} as a function of r and S_{cut} .

the scaling relations governing the external field. We defined the critical exponents δ and γ using S , p and r , which serve as analogues of the total magnetization, temperature and external field, respectively. The values of the critical exponents are universal and relate well with the known values previously obtained for standard percolation on a 2d lattice. Furthermore, we find that our

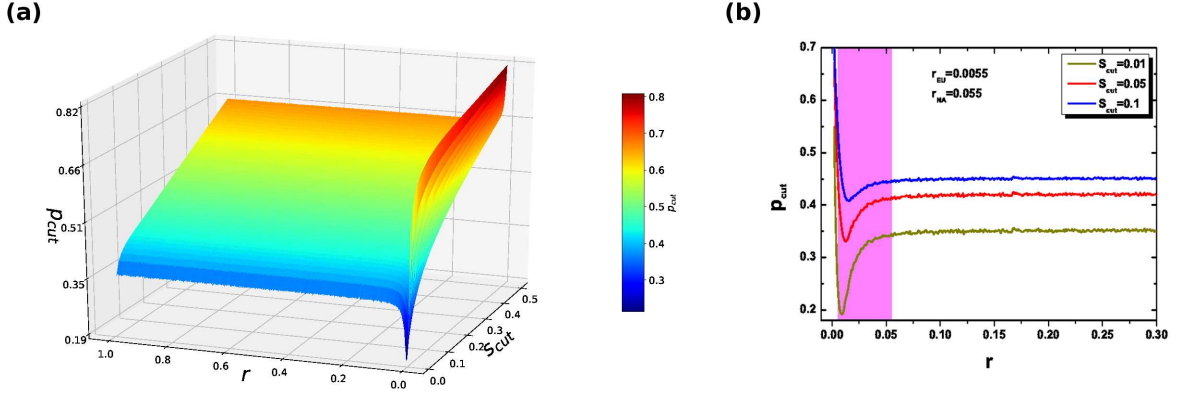


Figure 5. The effective percolation threshold for a real-world network. (a) p_{cut} as a function of r and S_{cut} . (b) p_{cut} as a function of r with $S_{cut} = 0.01, 0.05, 0.1$. The region between $r_{EU} = 0.0055$ and $r_{NA} = 0.05$ is highlighted.

scaling relations obey the Widom's identity.

We next defined the effective percolation threshold to quantify the robustness of our model. We found that there exists an optimal amount of interconnected nodes, which is also predicted and observed in real-world networks. Our approach provides a new perspective on resilience of networks with community structure and gives insight on its interlinks response as an external field. Lastly, our model provides a method for optimizing real world interconnected infrastructure networks which could be implemented by practitioners in the field.

ACKNOWLEDGEMENTS

We acknowledge the Israel-Italian collaborative project NECST, the Israel Science Foundation, the Major Program of National Natural Science Foundation of China (Grants 71690242, 91546118), ONR, Japan Science Foundation, BSF-NSF, and DTRA (Grant no. HDTRA-1-10-1-0014) for financial support. This work was partially supported by National Natural Science Foundation of China (Grants 61403171, 71403105, 2015M581738 and 1501100B) and Key Research Program of Frontier Sciences, CAS, Grant No. QYZDJ-SSW-SYS019. J.F thanks the fellowship program funded by the Planning and Budgeting Committee of the Council for Higher Education

of Israel.

- [1] Gao, J., Barzel, B. & Barabási, A.-L. Universal resilience patterns in complex networks. *Nature* **530**, 307–312 (2016). URL <http://www.nature.com/nature/journal/v530/n7590/abs/nature16948.html>.
- [2] Cohen, R., Erez, K., ben Avraham, D. & Havlin, S. Resilience of the Internet to Random Breakdowns. *Physical Review Letters* **85**, 4626–4628 (2000). URL <http://link.aps.org/doi/10.1103/PhysRevLett.85.4626>.
- [3] Albert, R., Jeong, H. & Barabási, A.-L. Error and attack tolerance of complex networks. *Nature* **406**, 378 (2000).
- [4] Tanizawa, T., Paul, G., Cohen, R., Havlin, S. & Stanley, H. E. Optimization of network robustness to waves of targeted and random attacks. *Physical Review E* **71**, 047101 (2005).
- [5] Buldyrev, S. V., Parshani, R., Paul, G., Stanley, H. E. & Havlin, S. Catastrophic cascade of failures in interdependent networks. *Nature* **464**, 1025–1028 (2010). URL <http://www.nature.com/nature/journal/v464/n7291/full/nature08932.html>.
- [6] Leicht, E. A. & D’Souza, R. M. Percolation on interacting networks. *arXiv:0907.0894 [cond-mat]* (2009). URL <http://arxiv.org/abs/0907.0894>. ArXiv: 0907.0894.
- [7] Hu, Y., Ksherim, B., Cohen, R. & Havlin, S. Percolation in interdependent and interconnected networks: Abrupt change from second- to first-order transitions. *Physical Review E* **84**, 066116 (2011). URL <https://link.aps.org/doi/10.1103/PhysRevE.84.066116>.
- [8] Gao, J., Buldyrev, S. V., Havlin, S. & Stanley, H. E. Robustness of a network of networks. *Physical Review Letters* **107**, 195701 (2011).
- [9] Gao, J., Buldyrev, S. V., Stanley, H. E. & Havlin, S. Networks formed from interdependent networks. *Nature Physics* **8**, 40–48 (2012). URL <http://www.nature.com/nphys/journal/v8/n1/full/nphys2180.html>.
- [10] Shekhtman, L. M., Shai, S. & Havlin, S. Resilience of networks formed of interdependent modular networks. *New Journal of Physics* **17**, 123007 (2015).

- [11] Hackett, A., Cellai, D., Gmez, S., Arenas, A. & Gleeson, J. Bond Percolation on Multiplex Networks. *Physical Review X* **6**, 021002 (2016). URL <https://link.aps.org/doi/10.1103/PhysRevX.6.021002>.
- [12] Sol-Ribalta, A., Gmez, S. & Arenas, A. Congestion Induced by the Structure of Multiplex Networks. *Physical Review Letters* **116**, 108701 (2016). URL <https://link.aps.org/doi/10.1103/PhysRevLett.116.108701>.
- [13] Stauffer, D. & Aharony, A. *Introduction to percolation theory* (Taylor & Francis, 2003).
- [14] Bunde, A. & Havlin, S. *Fractals and disordered systems* (Springer Science & Business Media, 2012).
- [15] Saberi, A. A. Recent advances in percolation theory and its applications. *Physics Reports* **578**, 1–32 (2015).
- [16] Li, D. *et al.* Percolation transition in dynamical traffic network with evolving critical bottlenecks. *Proceedings of the National Academy of Sciences* **112**, 669–672 (2015).
- [17] Meng, J., Fan, J., Ashkenazy, Y. & Havlin, S. Percolation framework to describe El Nino conditions. *Chaos: An Interdisciplinary Journal of Nonlinear Science* **27**, 035807 (2017). URL <http://aip.scitation.org/doi/abs/10.1063/1.4975766>.
- [18] Dong, G. *et al.* Resilience of networks with community structure behaves as if under an external field. *Proceedings of the National Academy of Sciences* **in press** (2018).
- [19] Weiss, D. J. *et al.* A global map of travel time to cities to assess inequalities in accessibility in 2015. *Nature* **553**, 333–336 (2018). URL <https://www.nature.com/articles/nature25181>.
- [20] Strano, E. *et al.* The scaling structure of the global road network. *Royal Society open science* **4**, 170590 (2017).
- [21] Hines, P., Blumsack, S., Sanchez, E. C. & Barrows, C. The topological and electrical structure of power grids. In *System Sciences (HICSS), 2010 43rd Hawaii International Conference on*, 1–10 (IEEE, 2010).
- [22] The global railway and airports data are from natural earth. <http://www.naturalearthdata.com/>. the airline routes data are from openflights. <https://openflights.org/data.html> .
- [23] Stanley, H. E. *Phase transitions and critical phenomena* (Clarendon, Oxford, 1971).
- [24] Reynolds, P., Stanley, H. & Klein, W. Ghost fields, pair connectedness, and scaling: exact results in one-dimensional percolation. *Journal of Physics A: Mathematical and General* **10**, L203 (1977).

- [25] Shai, S. *et al.* Critical tipping point distinguishing two types of transitions in modular network structures. *Physical Review E* **92**, 062805 (2015). URL <https://link.aps.org/doi/10.1103/PhysRevE.92.062805>.
- [26] Li, D., Qin, P., Wang, H., Liu, C. & Jiang, Y. Epidemics on interconnected lattices. *EPL (Europhysics Letters)* **105**, 68004 (2014).
- [27] Shekhtman, L. M. *et al.* Critical field-exponents for secure message-passing in modular networks. *New Journal of Physics* **20**, 053001 (2018). URL <http://stacks.iop.org/1367-2630/20/i=5/a=053001>.
- [28] Newman, M. E. J. & Ziff, R. M. Efficient Monte Carlo Algorithm and High-Precision Results for Percolation. *Physical Review Letters* **85**, 4104–4107 (2000). URL <https://link.aps.org/doi/10.1103/PhysRevLett.85.4104>.
- [29] *Supplementary materials* .
- [30] Domb, C. *Phase transitions and critical phenomena*, vol. 19 (Academic press, 2000).
- [31] Margolina, A., Herrmann, H. J. & Stauffer, D. Size of largest and second largest cluster in random percolation. *Physics Letters A* **93**, 73–75 (1982). URL <http://www.sciencedirect.com/science/article/pii/0375960182902195>.
- [32] Li, W., Bashan, A., Buldyrev, S. V., Stanley, H. E. & Havlin, S. Cascading Failures in Interdependent Lattice Networks: The Critical Role of the Length of Dependency Links. *Physical Review Letters* **108**, 228702 (2012). URL <https://link.aps.org/doi/10.1103/PhysRevLett.108.228702>.

Supplemental Materials: Resilience of spatial networks with inter-links behaving as an external field

Jingfang Fan, Gaogao Dong, Louis M. Shekhtman, Dong Zhou, Jun Meng, Xiaosong Chen and Shlomo Havlin

Appendix A: Further results

We present here some further results not given in the main text.

We consider two additional models with $\langle k_{inter} \rangle = 1$. For these models we randomly add $M_{inter} = rN_1$ inter-links between two lattice networks within a distance (i) $d = 0$ [as shown in Fig. S2(a)] and (ii) $d < \infty$ [as shown in Fig. S2(b)], the definition of d can refer in [32]. We repeat our analysis in these two new models and present the results in Fig. S3. We find that the critical exponents δ and γ are constant for these cases and do not change with $\langle k_{inter} \rangle$ and d . However, the optimization phenomenon is absent in both new models in terms of the effective percolation threshold [in Fig. S4].

In addition, we also study the external field effect on two ER networks with a fixed $\langle k_{inter} \rangle$. Distinct from our models, we find that the value of $\langle k_{inter} \rangle$ significantly influences the critical exponents: only for large $\langle k_{inter} \rangle$ are Eqs. (1) and (2) satisfied with the mean-field values $\delta = 2$, $\gamma = 1$ [18] [see Fig. S5]. The origin of such difference is that, for smaller $\langle k_{inter} \rangle$, the external field is not strong enough to distinguish the percolation threshold for different r [see Fig. S5(b)]. In contrast it is easy to distinguish the changes from varying r with large $\langle k_{inter} \rangle$ [see the Fig. S5(a)].

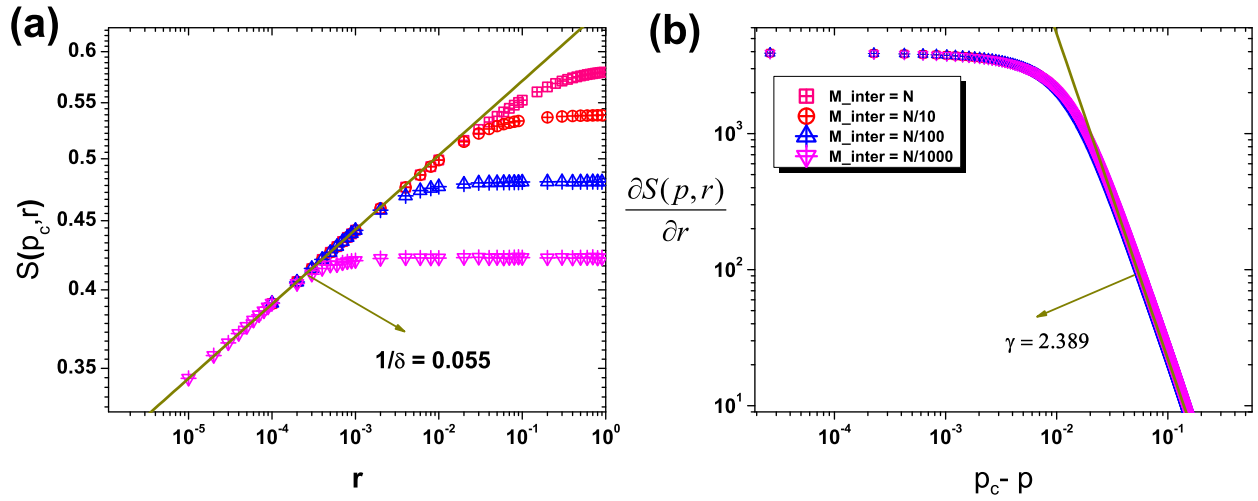


Figure S1. (a) $S(p_c, r)$ as a function of r for different M_{inter} . (b) $\frac{\partial S(r, p)}{\partial r}$ as a function of $p_c - p$ for $r = 10^{-4}$ and different M_{inter} . The solid green lines in (a) and (b) show the slope $1/\delta = 0.055$ and $\gamma = 2.389$ respectively.

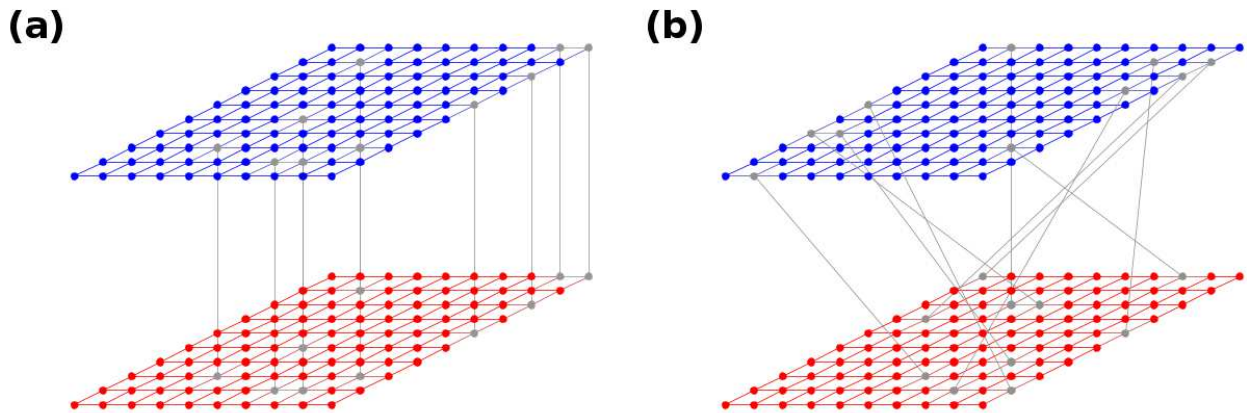


Figure S2. Our model with $\langle k_{inter} \rangle = 1$ and $r = 0.1$ for (a) $d = 0$ and (b) $d < \infty$.

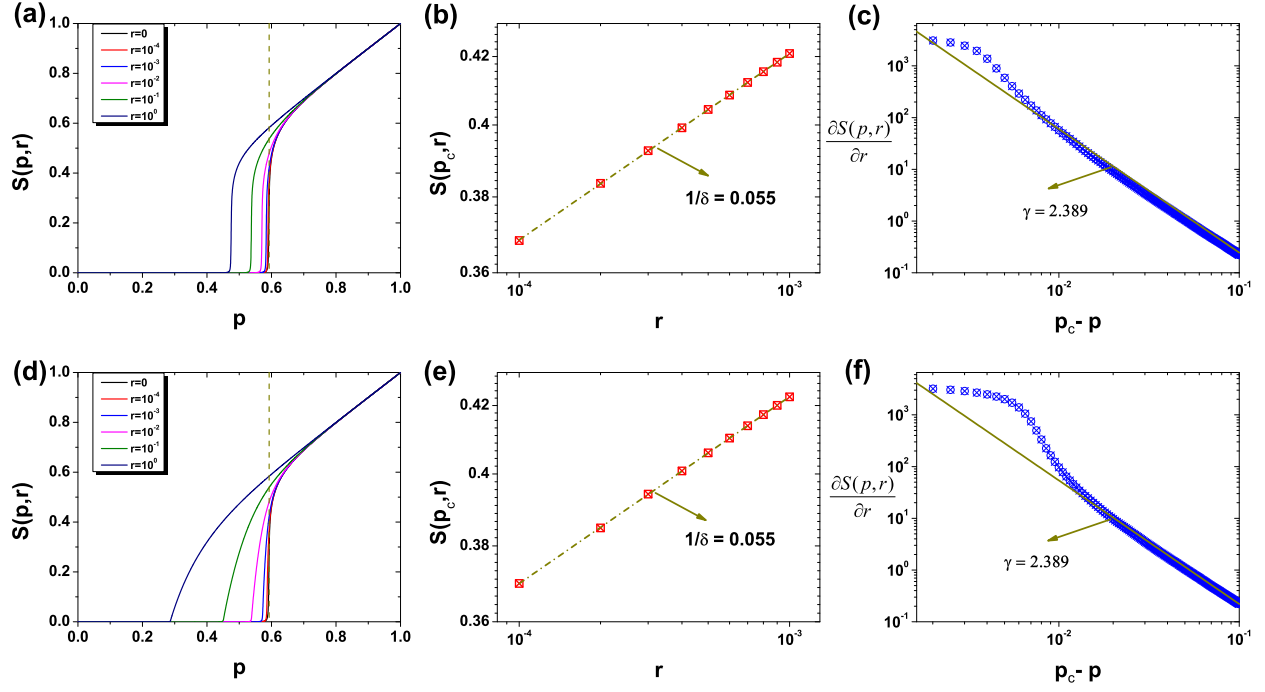


Figure S3. Similar to Fig. 2 from the main text but for the additional models with $\langle k_{inter} \rangle = 1$ and (a)(b)(c) the distance $d = 0$, (d)(e)(f) $d < \infty$.

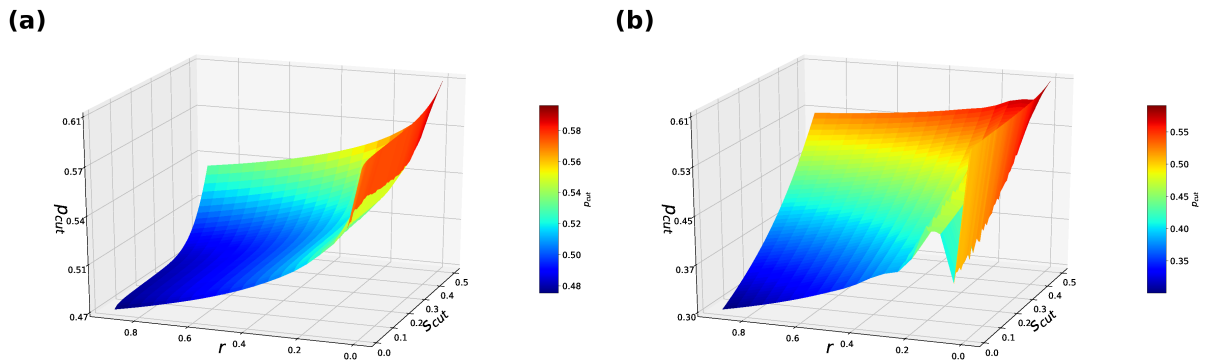


Figure S4. Effective percolation threshold for the additional models with $\langle k_{inter} \rangle = 1$ and (a) $d = 0$, (b) $d < \infty$.

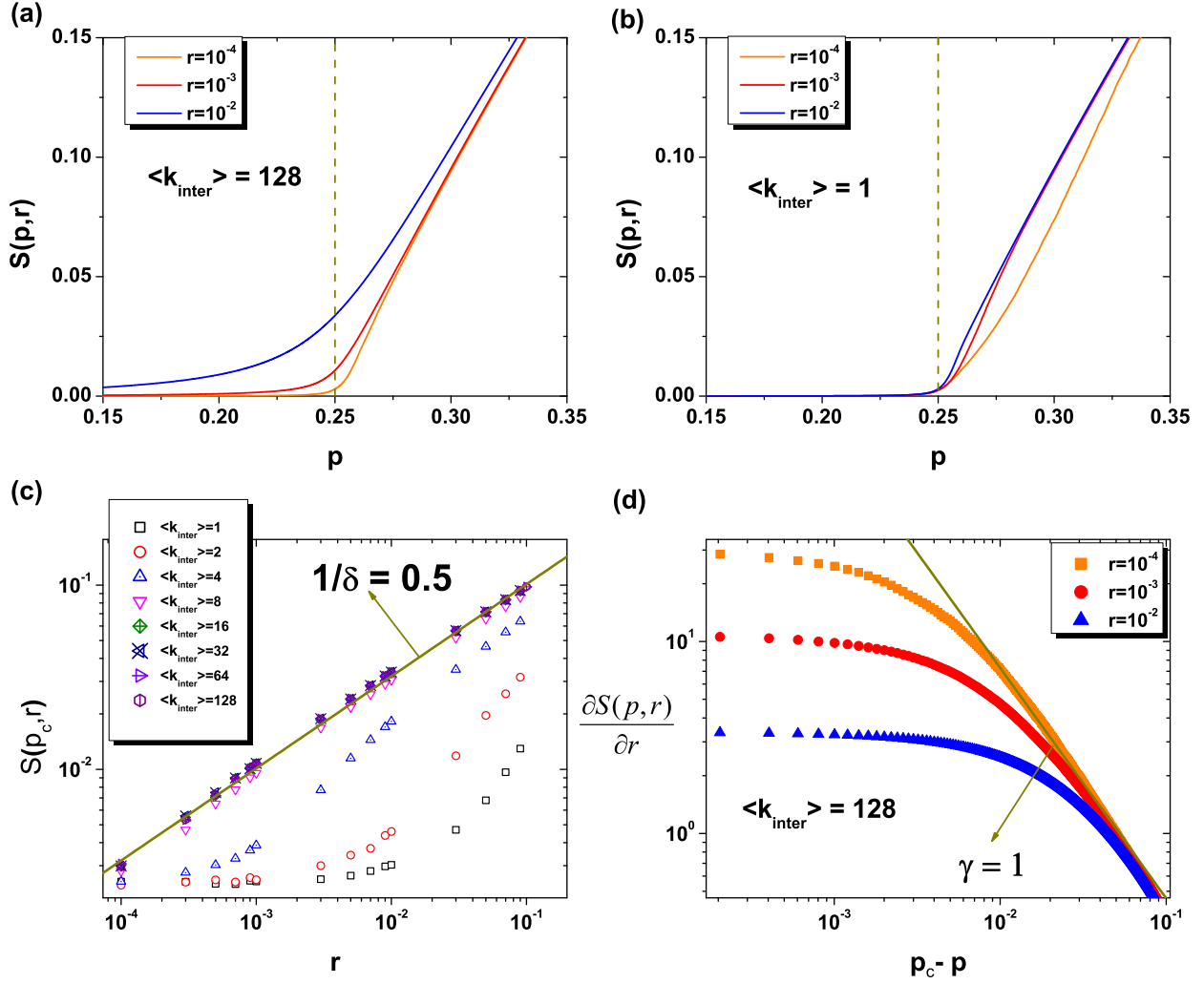


Figure S5. The size of the giant component $S(p, r)$ of two interconnected ER networks as a function of p for varying r with: (a) $\langle k_{inter} \rangle = 128$ and (b) $\langle k_{inter} \rangle = 1$. (c) $S(p_c, r)$ as a function of r for varying $\langle k_{inter} \rangle$. (d) $\frac{\partial S(p, r)}{\partial r}$ as a function of $p_c - p$ with $\langle k_{inter} \rangle = 128$. The average degree for each individual ER network is $\langle k \rangle = 4$ for all plots. The vertical dashed lines in (a) and (b) show the critical threshold for a single ER network, $p_c = 1/\langle k \rangle = 0.25$. The solid green lines in (c) and (d) show the slope $1/\delta = 0.5$ and $\gamma = 1$, respectively.